MgO(001) surface phonons from *ab initio* calculations

Vladimir Shpakov,[1,2] Anders Gotte,[1] Micael Baudin,[1] Tom Woo,[2] and Kersti Hermansson[1]
[1]*Materials Chemistry, The Ångström Laboratory, Uppsala University, Box 538, S-751 21 Uppsala, Sweden*
[2]*Department of Chemistry, University of Western Ontario, London, Ontario, Canada N6A 5B7*
(Received 10 June 2005; published 23 November 2005)

An *ab initio* study of the surface phonons in high-symmetry points of the Brillouin zone has been performed for the clean MgO(001) surface in the framework of the density functional theory (DFT) using plane waves and a lattice-dynamical treatment with a supercell approach. It is found that a calculation of the surface phonon modes using the DFT is a competitive approach compared to earlier shell-model calculations in the literature. The strongly localized phonon modes can be calculated with a reasonable accuracy using thin slab systems and a modest plane-wave cutoff.

DOI: 10.1103/PhysRevB.72.195427 PACS number(s): 68.35.−p

I. INTRODUCTION

The *ab initio* investigation of phonons on defective and nondefective oxide surfaces is of current interest in heterogeneous catalysis. Many commercially important catalytic surface reactions take place at an elevated temperature, where the adsorbate-surface interactions are influenced by the substrate's surface vibrations. It is known that the localized surface vibrations are very sensitive to the presence of adsorbates.[1,2] Conversely, the adsorption at the different surface sites depends on the characteristics of the low-frequency vibrations of the adsorbate molecules,[2] where couplings with low-frequency substrate phonons will affect these vibrations. Moreover, some surface phonons will give rise to rather distorted transient surface structures, which should lead to altered adsorbate-surface interactions compared to those of a static, relaxed structure. In summary, it is clear that the surface phonons play a complex and crucial role in the context of molecule-surface interactions and molecular reactions on surfaces, but the detailed mechanisms for this interplay are not known. Accurate knowledge about the clean-surface phonons and about the viable methods to compute these is an important step towards a more complete surface characterization of the dynamical effects on the molecule-surface interactions.

Ab initio calculations based on density functional theory (DFT) nowadays represent a mature and computationally feasible approach to investigating properties of condensed bulk matter and the method sometimes constitutes a viable (or even superior) alternative to classical force-field simulations using, for example, the shell model[3] for the metal oxides. The present paper deals with surfaces and describes *ab initio* calculations of the lattice dynamics (LD) of the MgO(001) surface. A characterization of the phonon modes is given and their surface localization is discussed.

A number of theoretical *ab initio* investigations of surface electronic structure,[6] surface relaxation,[7] defect energetics,[8] and water adsorption[9–11] on MgO surfaces have been published. Successful *ab initio* studies of the lattice dynamics of bulk MgO have been performed using density-functional perturbation theory[12] (DFPT) and frozen-phonon calculations.[8] As far as the surface dynamics of MgO is concerned, shell-model simulation results were presented decades ago for the unrelaxed[13] and the relaxed[14] (001) surface. The shell model parameters used in Refs. 13 and 14 reproduce the experimental bulk dispersion curves well.[4] More recently, the "environmentally dependent" set of shell-model (EDSM) parameters was proposed,[5] based on *ab initio* MgO cluster relaxation calculations. This set was employed in Ref. 15 for the interpretation of the experimental phonon density of states (DOS) for MgO nanocrystals as measured by the neutron scattering technique,[16,17] but no description of the surface phonons was presented.

This paper is organized as follows. Section II gives a short outline of the theory and thereafter the computational details and the testing of some aspects of these theories are presented. In Sec. III we give the main results and a comparison with experimental data. The paper ends with a short summary.

II. METHOD

A. Analytical background

The electronic structure calculations for the MgO(001) surface have been performed here for a system consisting of identical thin slabs repeated periodically in the direction perpendicular to the slab surfaces. In such a model, neighboring slabs have to be separated by a vacuum gap of sufficient thickness to exclude interaction. Under such conditions, the dynamics of a single slab and of the periodic slab system are essentially the same.

In the traditional frozen-phonon scheme, the dynamical matrix of the system is determined by displacing an atom α, and all its periodic images, from their equilibrium positions by the amount

$$U_{l\alpha j} = \frac{1}{\sqrt{M_\alpha}} V_{\alpha j} \exp\{i\vec{q}\vec{R}_l\}, \tag{1}$$

where l denotes the lth primitive cell, $\vec{R}_l$ is the corresponding translation vector, M_α the mass of atom α, and $V_{\alpha j}$ is the jth component of the phonon polarization vector in a given $\vec{q}$ point of surface Brillouin zone. All other atoms are at their equilibrium positions. The ith component of the harmonic force acting on any atom β in the 0th primitive cell is

$$F_{0\beta i} = -\sum_{\alpha j} \sqrt{M_\beta}\, D_{ij}(\beta\alpha,\vec{q}) V_{\alpha j}, \tag{2}$$

where a dynamical matrix element D_{ij} is a sum defined as

$$D_{ij}(\beta\alpha,\vec{q}) = \frac{1}{\sqrt{M_\beta M_\alpha}} \sum_l \phi_{ij}(0\beta,l\alpha)\exp\{i\vec{q}\vec{R}_l\} \tag{3}$$

and $\phi_{ij}(0\beta,l\alpha)$ is a force constant matrix element. By choosing the appropriate displacement patterns, each with a wave vector $\vec{q}$, the dynamical matrix $D(\beta\alpha,\vec{q})$ can be determined for different $\vec{q}$ points in the surface Brillouin zone (for a detailed description, see Ref. 18). This procedure requires that the atomic displacements in the supercell fulfill the following condition:

$$\exp\{i\vec{q}\vec{R}_L\} = 1, \tag{4}$$

where $\vec{R}_L$ is any translation vector of the supercell. If (4) is fulfilled, the displacements (1) will be periodic with the period of the supercell.

It is not always convenient to consider many different supercells. Instead we can use a big enough supercell and only consider the Γ point. Equation (2) applied to the analytical part of the dynamical matrix of the supercell, $D^{\text{supercell}}(\beta\alpha,\vec{q}=0)$, becomes

$$F_{0\beta i} = -\sum_{\alpha j} \sqrt{M_\beta}\, D_{ij}^{supercell}(\beta\alpha,\vec{q}=0) V_{\alpha j}, \tag{5}$$

where we have the same atomic displacements in the supercell and its periodically repeated images. For those $\vec{q}$ points which satisfy condition (4) above we can write

$$D_{ij}(\beta\alpha,\vec{q}) = \sum_l D_{ij}^{supercell}(\beta\alpha_l,\vec{q}=0)\exp\{i\vec{q}\vec{R}_l\} \tag{6}$$

where l denotes the various cells within the supercell and α_l is the periodic image of atom α in cell l. Equation (6) can be deduced from condition (4), the fact that the supercell translation vectors $\vec{R}_L$ are some combinations of the primitive cell translation vectors $\vec{R}_l$, and the definition of the dynamical matrix (3). The dynamical matrix in (6) can then be used in the calculation of the phonon frequencies and polarization vectors in the standard way,[19] by solving

$$\omega^2 V_{\beta i} = \sum_{\alpha j} D_{ij}(\beta\alpha,\vec{q}) V_{\alpha j} \tag{7}$$

which gives $3n$ eigenvalues ω^2 and the corresponding $3n$ eigenvectors $V_{\alpha j}$ in any $\vec{q}$ point.

This simple procedure yields the exact dynamical solution for a finite number of Brillouin zone points of the primitive cell, namely those points which have wave vectors which are commensurate with the reciprocal lattice vectors of the supercell. We have used this method to calculate the phonons in selected surface Brillouin zone points of MgO(001).

Note that, according to formulas (5) and (6), only the displacements of atoms within the primitive cell are required. The use of symmetry can further decrease the number of displacements needed.[20] Equations (5) and (6) are related to the force constant-based *ab initio* procedure employed in Ref. 20 for diamond and graphite, which can be seen if the primitive cell is placed in the middle of the supercell and Eq. (6) is extrapolated to any $\vec{q}$ value.

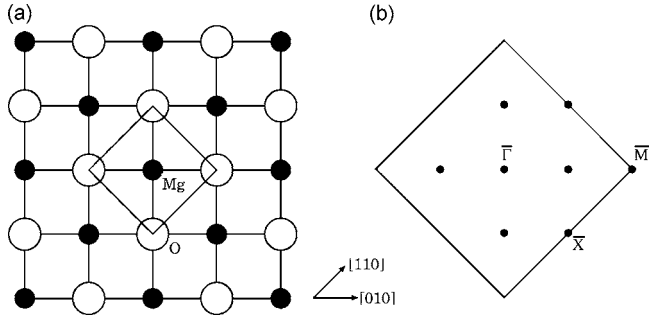

FIG. 1. A schematic picture of the MgO(001) surface in the *xy* plane. (a) The 2×2 supercell in real space, with the primitive cell marked. (b) The Brillouin zone in reciprocal space, with the eight reciprocal points (four of them unique) investigated.

Compared to the traditional frozen-phonon scheme, the advantage of this technique is that only a very small set of calculations within the given supercell is sufficient to determine the dynamical matrix. The main limitation of the approach lies in the size of the supercell.

B. Computational details

All energy and force calculations were performed within the density-functional framework[21] with the gradient-corrected PBE functional,[22] in combination with the two-electron and six-electron norm-conserving pseudopotentials of the Goedecker type[23] for Mg and O, respectively. The plane-wave-based CPMD code[24] was used.

Bulk calculations were performed with a supercell constructed from $2\times2\times2$ crystallographic unit cells, containing 64 ions. The MgO(001) surface calculations were done with two different slab systems: one four-layer system and one eight-layer system, both containing eight Mg and eight O ions in each layer. The simulation boxes were repeated in three dimensions. In both cases, the surfaces were separated by a vacuum gap with the same thickness as the oxide slab. The supercell dimensions were thus $8.42\times8.42\times16.84$ Å^3 for the thin slab system and $8.42\times8.42\times33.68$ Å^3 for the thick slab system.

The supercell and the surface Brillouin zone are shown in Fig. 1. The size of the supercell allows us to investigate the vibrational modes at four unique points of the Brillouin zone, including the high-symmetry points $(\bar{\Gamma},\bar{X},\bar{M})$. The Brillouin zone integrations for the electronic system in the supercell were carried out using only the $\bar{\Gamma}$ point. To ensure satisfactory frequency convergence a larger real-space mesh than the CPMD default value was used for the fast fourier transform (FFT) calculations. The LD calculations for the bulk and for the thin slab were performed using three different plane-wave cutoff values (100, 120, and 140 Ry) to investigate the phonon frequency convergence with respect to cutoff. The frequencies calculated for the bulk with 140 and 120 Ry cutoffs differed by less than 1%, and the same or still better convergence was observed in the slab calculations. Between

TABLE I. Phonon frequencies (in THz) calculated at the high-symmetry points compared with the experimental Γ, X, M, for MgO bulk, compared with the experimental data and published calculations using density-functional perturbation theory.

	DFPT[a]	Expt.[b]	Our results
Γ TO	11.72	12.23	11.58
X TA	8.62	8.96	8.77
X LA	12.59	12.65	12.59
X TO	13.37	13.29	13.52
X LO	16.55	16.61	17.1
L TA	8.20	8.64	8.18
L LA	16.40		16.4
L TO	10.71	11.05	10.74
L LO	17.07		17.55

[a]Reference 12.
[b]References 4 and 26.

140 and 100 Ry, the frequencies of the strongly localized surface phonons S_1, S_4, and S_5 (see later) differed by only 2–3 %. The results discussed below were calculated using the following cutoffs: 140 Ry for the bulk, 140 Ry for the thin slab, and 100 Ry for the thick slab.

As a test of the accuracy of the strategy employed, we performed geometry optimizations of the MgO molecule and of bulk MgO. The optimization for the isolated MgO molecule gave a bond length of 1.75 Å and a Mg—O harmonic stretching frequency of 770 cm^{-1}, which agree well with the experimental values 1.75 Å and 756 cm^{-1} (Ref. 25). For bulk MgO, the optimized lattice constant was 4.225 Å. This is also close to the experimental value of 4.21 Å. All calculations presented in this paper used the experimental bulk cell parameter.

The results of the *ab initio* LD calculations for bulk MgO at the highest plane-wave cutoff are presented in Table I for the high-symmetry points in the Brillouin zone and compared with results from the DFPT calculation of Schütt *et al.*[12] (LDA calculations with the norm-conserving Troullier-Martins pseudopotentials) and also with the experimental data of Sangster *et al.*[4] and Jasperse *et al.* [26] Table I shows the overall agreement of our results with the available optical and neutron scattering data. Our results lie within 4–6 % of the experimental frequencies. These results give confidence that the method used here has a high predictive power, also when applied to experimentally unknown features of MgO surface phonons.

III. RESULTS AND DISCUSSION

A. Phonon description

For diatomic ionic crystals like MgO, there exist six phonon branches, namely one longitudinal-optical (LO), one longitudinal-acoustical (LA), two transverse-optical (TO), and two transverse-acoustical (TA), which give rise to rather broad DOS peaks with maxima as indicated by the vertical dotted lines in Figs. 2 and 3. In lattice-dynamical slab calculations, surface modes appear in quasidegenerate pairs, where one member is localized at one surface and the other member at the other surface. In Ref. 13, a labeling convention for different types of surface modes was proposed, where modes were assigned a label $S_i (i=1,2,\ldots,8)$. We have adopted the same notation as in Ref. 13.

The phonon modes in the slab systems were analyzed using the local frequency spectrum (LFS) function,[27] which was calculated for all atoms in the slab using the available eigenvalues and eigenvectors of the dynamical matrix [Eq. (7)], according to the formula

TABLE II. Calculated frequencies (in THz) for MgO(001) slab surface modes S_1-S_7 at high-symmetry points $\bar{\Gamma}$, $\bar{X}$, and $\bar{M}$ for the thin (four layers) and thick (eight layers) slab systems. Results from experiment and from shell-model calculations are shown for comparison.

		Shell model[a]	Thin slab	Thick slab	Expt.
$\bar{\Gamma}$	$S_{4,5}$	10.9	11.49-11.62	10.86	10.5[b,c], 10.9[d]
	S_2		14.62-15.11	14.8-14.95	~15[b,c], 15.75[e,f]
$\bar{X}$	S_3	17.48	16.82	15.77	
	S_5	9.25	9.37	9.34	
	S_4	9.76	9.02	9.40	
	S_7	8.44	7.63	7.76	
	S_1'	7.90			
	S_1	6.94	7.26	7.24	7.3
$\bar{M}$	S_1'		8.32	8.38	
	S_1	8.16	7.48	7.41	

[a]Reference 14.
[b]Reference 16.
[c]Reference 17.
[d]Reference 29.
[e]Reference 28.
[f]Reference 31.

$$Z_\alpha(\omega) = \frac{1}{3N} \sum_{modes\ k} |\vec{V}_{\alpha,k}|^2 \delta(\omega - \omega_k). \quad (8)$$

In Eq. (8), $|\vec{V}_{\alpha,k}|^2$ is the sum of the squares of the polarization vector components for atom α in mode k, N is the number of atoms in the supercell, and the sum is calculated over all 192 (384) modes for the thin (thick) slab. The LFS function provides a quantitative measure of the contributions of a particular atom to the vibrations in a given frequency region, averaged over the x, y, and z directions. For the thin slab system, the LFS function was first averaged over the two outermost oxide layers (one on each side) and then over the two internal layers. The difference between these averaged LFS functions for the surface and the internal layers, i.e.

$$\Delta Z(\omega) = Z_{\text{surface}}(\omega) - Z_{\text{interior}}(\omega), \quad (9)$$

is presented in Fig. 2. A large positive value for the difference function $\Delta Z(\omega)$ pinpoints the existence of a surface phonon. For the thick slab, averaging was performed over the two outermost layers (one on each side) and also over the two second outermost layers (one on each side), and over the four internal layers. The resulting difference functions are presented in the upper and lower parts, respectively, of Fig. 3. Moreover, a careful analysis of each phonon mode in terms of its polarization vectors allowed us to characterize each surface phonon according to the definitions in Ref. 13. In the following, these phonon modes are discussed.

1. Thin slab model

The values of the calculated frequencies at the high-symmetry points for the thin slab are presented in Table II. For the thin (001) slab, going from left to right in Fig. 2, we have, at first, in the low-energy part of the spectrum, some modes which have large surface contributions, but which are not located at the high-symmetry points in the two-dimensional Brillouin zone. These phonons, at approximately 5.5 and 8.5 THz (R_1, R_2, and R_3), are located at $\overline{\Gamma M}/2$. In R_1, and R_2, the magnesium atoms vibrate perpendicularly to the surface, in R_3 the Mg atom vibrations are parallel to the surface. The next peak is marked S_1, because it corresponds to the $\overline{X}$ point of the S_1 phonon branch. This peak is a truly localized phonon in our slab system and consists of a shear-horizontal (SH) Mg vibration, polarized perpendicular to the plane formed by the surface normal and the wave vector, i.e., both the propagation direction and the ionic displacements lie in the xy plane. The next peak shows another S_1 phonon; this one corresponds to the $\overline{M}$ point of the S_1 phonon branch, where the Mg atoms vibrate in the z direction. The next phonon with a large surface contribution is S_1', where the oxygen atoms vibrate in the z direction; this phonon is also located at the $\overline{M}$ point. Above the frequency of the bulk TA peak (dotted line), we observe an S_4 surface phonon at the $\overline{X}$ point, with the O atoms vibrating in the z direction. The next peak is related to the S_5 phonon at the $\overline{X}$ point, with O atom vibrations of the SH type. The split peaks at 11.5 THz and 14.8 THz are connected to the S_4, S_5, and S_2 phonons at the $\overline{\Gamma}$ point; these modes have their origins in the TO and LO bulk bands. The comparatively large splitting for these phonons is due to the small thickness of this slab.

For the thin slab in Fig. 2 some of the peaks are seen to be lower (less surface localized) than others. This is, for example, true for the S_2 peak (at ~15 THz) and the S_7 peak (at ~7.6 THz), where the Mg atoms vibrate in the z direction, and for the S_3 phonon (at ~15.8 THz), where the O atoms vibrate in the xy plane and in the same direction as the wave vector; the latter two are observed at the $\overline{X}$ point. Most of the surface modes for the thin slab in Fig. 2, but not all, remain as surface modes when the slab is made thicker. This is shown in Fig. 3 and will be discussed in more detail below.

2. Thick slab model

The calculations with the thick slab (Fig. 3) show that the the S_1 and S_7 phonons at the $\overline{X}$ point and the S_1 and S_1' phonons at the $\overline{M}$ point change very little as the thickness increases. They remain surface localized modes and their frequencies change very little. The frequencies of the S_4 and S_5 phonons at the $\overline{\Gamma}$ point move to slightly lower values and the splitting of the S_4, S_5 phonon pair disappears. The S_2 mode at the $\overline{\Gamma}$ point moves to a slightly higher frequency for

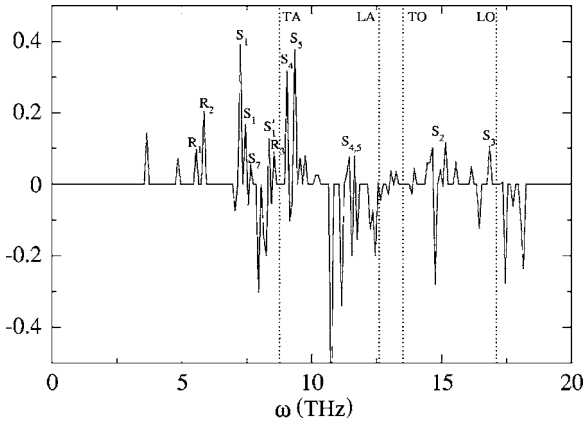

FIG. 2. $\Delta Z(\omega)$ as defined in Eq. (9), calculated for the thin slab system. The dotted lines refer to the bulk calculations.

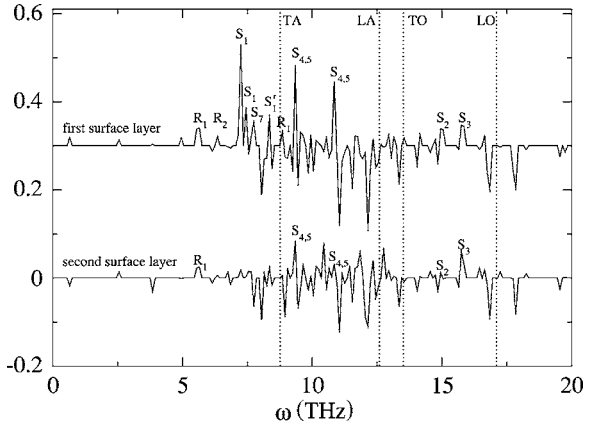

FIG. 3. $\Delta Z(\omega)$ for the thick slab system. Upper plot: the surface region is considered to be the outermost layer on each side. Lower plot: the surface region is considered to be the second outermost layer on each side.

our thicker slab calculation, and some small splitting remains for the S_2 mode. The frequency of the longitudinal S_3 phonon decreases when the slab is made thicker. The so-called macroscopic phonons (S_1, S_1', S_7) (see, for example, Ref. 13 for a definition of macroscopic and microscopic modes), and the microscopic S_4, S_5 modes at the $\bar{\Gamma}$ point are strongly localized in the first surface layer, as is clearly seen from a comparison of the two graphs in Fig. 3. However, the peaks originating from the S_4, S_5, and S_3 microscopic surface phonon modes at the $\bar{X}$ point are seen to have significant intensity at both in the lower and upper graphs in Fig. 3, implying that their vibrations are distributed over two surface layers. The analysis of the eigenvector components for the S_2 phonon mode reveals a comparatively large contribution from the internal layers, which suggests that the S_2 surface phonon has considerable contributions from bulk atoms, and is therefore not a truly localized surface mode.

3. Comparison with shell-model results

In Table II our calculated frequencies are compared with literature values from shell-model calculations for a relaxed MgO(100) slab.[14] Overall, the results are in reasonable agreement. It is not our intention to attempt to claim that the DFT lattice-dynamical results are superior to the shell-model results; the present investigation simply provides an alternative and parameter-free route to calculating surface phonon frequencies for MgO(100).

One can note the following: (i) At the $\bar{X}$ point, the thick-slab DFT frequencies and the shell-model frequencies lie within about ±10% from each other, (ii) at the $\bar{\Gamma}$ point we find a mode (S_2) which is not present in the shell-model analysis, and (iii) in the shell-model investigation, the S_1' mode is assigned to the $\bar{X}$ point and not to the $\bar{M}$ point, as we find here. In the next section, our DFT-derived frequencies are compared with experimental results.

B. Comparison with experiment

Our results can be compared with the inelastic neutron scattering experiments of Rieder and Hörl for nanocrystals in Refs. 16 and 17. Their plots of the surface *minus* bulk excess DOS show four peaks (some of them quite broad), centered around 7, 10.5, 15, and 19 THz, respectively. The positions of our macroscopic TA surface phonons S_1, S_1', S_7 are in excellent agreement with their first peak (see Table II). Our S_4, S_5 pair at the $\bar{X}$ point lies about 1 THz below the second experimental peak maximum. Such a discrepancy does not necessarily imply a large disagreement, since our calculations were made in the harmonic approximation, while the neutron measurements were performed at 800 K. Recent MD simulations of ours at 300 K, using the same supercell as in the present LD study, shifts the 9.5 THz peak from the LD calculation to 10 THz. These and other details of the MD simulations will be published elsewhere.

The high-frequency mode at ~19 THz (a Fuchs-Kliever mode) observed in the inelastic neutron scattering measurements has also been observed in several electron energy loss spectroscopy (EELS) and high resolution electron energy loss spectroscopy (HREELS) experiments for single-crystal MgO(100) surfaces.[28–30] Recent HREELS measurements of thin and ultrathin MgO(100) films grown on Ag(100) also showed this phonon peak.[31] The Fuchs-Kliever mode is not observed in our calculations. Wassermann and Rieder[15] have argued that the presence of the two high-frequency peaks is related to the finite size of the crystals used in the experiments and therefore cannot be reproduced by two-dimensional infinite slab calculations.

The situation for the neutron-scattering-determined peak at 15 THz is controversial. This peak coincides with the phonon peak measured at 15.75 THz at the $\bar{\Gamma}$ point in the EELS experiment[28] for a single crystal with the sample cleaved in ultrahigh vacuum. In Ref. 28 the peak was assigned to an S_2 mode. Our related S_2 phonon frequency at the $\bar{\Gamma}$ point lies slightly lower. It so happens that our frequency for the S_3 phonon, calculated for the thick slab, coincides with the experimental peak of Ref. 28. The situation is further complicated by the fact that some other EELS (HREELS) experiments reported in the literature for cleaved MgO single crystals[29,30] do not report any mode at 15–16 THz.

Concerning the discrepancies among the various experiments, they appear to be small as far as the macroscopic surface phonons (S_1, S_1', S_7) are concerned. In contrast, the microscopic surface modes (all the other S_i modes) display discrepancies depending on the sample preparation method. So, for example, the only microscopic surface mode observed by Cox and Williams[29] was the S_4 (Lucas mode) at 10.9 THz in measurements carried out for an air-cleaved single crystal. When a secondary electron gun was used to prevent charging-up, no microscopic phonon was detected.[30] We suggest that the EELS results[28,29] with the successful observation of the macroscopic acoustic phonons (S_1, S_1', S_7) and microscopic S_4, S_5 phonons at the $\bar{\Gamma}$ point may be related to a strong localization of these modes to the first surface layer. The observation of the less surface-localized S_4, S_5 phonons (at the $\bar{X}$ point) may be easier to detect in the less surface-sensitive neutron experiments.

IV. SUMMARY AND CONCLUDING REMARKS

In summary, we have performed *ab initio* lattice dynamics calculations of the surface phonons of MgO(001). Our calculated frequencies are in reasonable agreement with available experimental data. Our results also show that strongly localized phonon modes, which should be the most important for the absorbate dynamics, can be calculated with reasonable accuracy using thin slab systems and a modest plane-wave cutoff.

We want to point out that DFT lattice-dynamical calculations do not necessarily out-perform force-field-based calculations in the general case, or even give results in closer agreement with experiment, since force-field-based methods can make use of larger systems and thus more $\bar{q}$ points, and, moreover, the force field can be tailored to perform well for the particular system under study, and even for the particular property under study. However, *ab initio* or DFT lattice-dynamical calculations are interesting because they can be used as an essentially parameter-free tool to derive surface

phonon properties, so that different systems can be treated on an equal (and quite high-level) footing. It is possible that in the future surface phonon frequencies obtained from *ab initio* calculations will provide valuable additional reference data for the determination of force-field parameters for classical surface simulations, because such parameters cannot be deduced unambiguously from fitting to bulk dispersion curves,[4] nor by fitting to surface relaxation data.[5]

DFT calculations for ionic bulk matter constitutes a mature field of computational condensed-matter theory. The present work shows that also surface phonon mode calculations using DFT give quite promising results, even for moderately sized surface systems. In future work, it will therefore be both feasible and interesting to explore larger and thicker computational cells, which will yield more information about the thickness dependence of the surface modes and will allow the exploration of more modes (dispersion curves) and more $\bar{q}$ points on the dispersion curves. It will also be important to further explore the possibilities and limitations of the DFT method itself and assess the sensitivity of the calculated surface lattice-dynamical data to the choice of functional and pseudopotential.

ACKNOWLEDGMENTS

Financial support from the Swedish Foundation for International Cooperation in Research and Education (STINT) and the Swedish Research Council (VR) are gratefully acknowledged as are the parallel computer resources provided within the SHARCNET project (Ontario). Useful discussions with Dr. Roger Rousseau (SISSA, Trieste) and Dr. Keith Refson (Rutherford Appleton Laboratory, UK) are much appreciated.

[1] K. Wolter, D. Scarano, J. Fritsch, H. Kuhlenbeck, A. Zecchina, and H.-J. Freund, Chem. Phys. Lett. **320**, 206(2000).
[2] G. Witte, Surf. Sci. **502-503**, 405 (2002).
[3] P. J. Mitchell and D. Fincham, J. Phys.: Condens. Matter **5**, 1031 (1993).
[4] M. J. L. Sangster, G. Peckham, and D. H. Saunderson, J. Chem. Phys. **3**, 1026 (1970).
[5] Ye Li, D. C. Langreth, and M. R. Pederson, Phys. Rev. B **55**, 16456 (1997).
[6] U. Schonberger and F. Aryasetiawan, Phys. Rev. B **52**, 8788 (1995).
[7] D. R. Alfonso, J. A. Snyder, J. E. Jaffe, A. C. Hess, and M. Gutowski, Phys. Rev. B **62**, 8318 (2000).
[8] A. De Vita, M. J. Gillan, J. S. Lin, M. C. Payne, I. Stich, and L. J. Clarke, Phys. Rev. B **46**, 12964 (1992).
[9] W. Langel and M. Parrinello, Phys. Rev. Lett. **73**, 504 (1994).
[10] L. Giordano, J. Goniakowski, and J. Suzanne, Phys. Rev. Lett. **81**, 1271 (1998).
[11] M. Odelius, Phys. Rev. Lett. **82**, 3919 (1999).
[12] O. Schütt, P. Pavone, W. Windl, K. Karch, and D. Strauch, Phys. Rev. B **50**, 3746 (1994).
[13] T. S. Chen, F. W. de Wette, and G. P. Alldredge, Phys. Rev. B **15**, 1167 (1977).
[14] W. Kress, F. W. de Wette, A. D. Kulkarni, and U. Schroder, Phys. Rev. B **35**, 5783 (1987).
[15] B. Wassermann and K. H. Rieder, Phys. Rev. Lett. **88**, 045501 (2002).
[16] K. H. Rieder and X. Hörl, Phys. Rev. Lett. **20**, 209 (1968).
[17] K. H. Rieder, Surf. Sci. **26**, 637 (1971).
[18] J. Fritsch, and U. Schroder, Phys. Rep. **309**, 209 (1999).
[19] A. A. Maradudin, E. W. Montroll, G. H. Weiss, and I. P. Ipatova, *Theory of Lattice Dynamics in the Harmonic Approximation*, Second Edition (Academic Press, New York, 1971).
[20] G. Kresse, J. Furthmuller, and J. Hafner, Europhys. Lett. **32**, 729 (1995).
[21] R. G. Parr and W. Yang, in *Density-Functional Theory of Atoms and Molecules* (Clarendon Press, Oxford 1989).
[22] J. P. Perdew, K. Burke, and M. Ernzerhof, Phys. Rev. Lett. **77**, 3865 (1996).
[23] C. Hartwigsen, S. Goedecker, and J. Hutter, Phys. Rev. B **58**, 3641 (1998).
[24] CPMD Version 3.5 developed by J. Hutter, A. Alavi, T. Deutsch, M. Bernasconi, St. Goedecker, D. Marx, M. Tuckerman, and M. Parrinello, Max Plank Institut für Festkorperforschung and IBM Zurich Research Laboratory, 1995–1999.
[25] S. N. Suchard, J. E. Meltzer, *Spectroscopic Data*, Vol. 1, *Heteronuclear Diatomic Molecules* (IFI/Plenum, New York 1975), Vol. 1.
[26] J. R. Jasperse, A. Kahan, J. N. Plendl, and S. S. Mitra, Phys. Rev. **146**, 526 (1966).
[27] P. H. Dederichs and R. Zeller, *Point Defect in Metals II*, Springer Tracts in Modern Physics, Vol. 87 (Springer-Verlag, New York, 1980).
[28] C. Oshima, T. Aizawa, R. Souda, and Y. Ishizawa, Solid State Commun. **73**, 45 (1990).
[29] P. A. Cox and A. A. Williams, J. Electron Spectrosc. Relat. Phenom. **39**, 45 (1986).
[30] P. A. Thiry, J. Ghijsen, R. Sporken, J. J. Pireaux, R. L. Johnson, and R. Caudano, Phys. Rev. B **39**, 3620 (1989).
[31] L. Salvio, E. Celasso, L. Vattuone, M. Rocca, and P. Senet, Phys. Rev. B **67**, 075420 (2003).